

Moderated Poster Session I

Friday, January 20, 2006

5:00 PM–6:30 PM

301. INCIDENCE OF ADVERSE EVENTS DURING CARDIAC MAGNETIC RESONANCE IMAGING IN CONGENITAL HEART DISEASE

Adam L. Dorfman, MD, Andrew J. Powell, MD, Kirsten C. Odegard, MD, Peter C. Laussen, MBBS, Tal Geva, MD. Children's Hospital Boston, Boston, MA, USA.

Introduction: Cardiac magnetic resonance imaging (CMR) is a diagnostic modality used increasingly in the evaluation of patients with congenital heart disease, in some cases to avoid catheterization and its attendant risks of morbidity. However, there is little published data on the incidence and types of adverse events (AEs) during CMR in this patient population.

Purpose: To describe the incidence of AE during CMR in this population, and to identify patient- or technique-related factors that predict the occurrence of AEs, which could help to avoid similar complications in the future.

Methods: Over a 26-month period, AEs were prospectively recorded in the clinical database for patients undergoing CMR at Children's Hospital Boston. This database was analyzed for patient and technical factors that could correspond to increased risk of AEs. Established hospital criteria were used by 3 independent observers to grade AEs on severity, preventability and attributability.

Results: There were 1334 studies identified (age range 1 day–75 years, median 15 years; 57% male.) Of these studies, there were 22 AEs (1.6%), all of which were transient. The AEs are classified in the table below:

Category of Adverse Event	n
Reaction or infiltrate related to gadolinium administration	9
Hypotension related to anesthesia, requiring pressors	6
Respiratory problems related to anesthesia	5
Reaction related to non-anesthesia medication (adenosine, glycopyrrolate)	2

On a severity scale of 1–5, 14 AEs (64%) were categorized as 1 or 2 (minor severity), 7 (32%) were categorized as 3 (moderate severity) and 1 (4.5%) was categorized as 4 (major severity). Three AEs (14%) were found to be possibly or definitely preventable, and 19 (86%) were definitely attributed to the performance of the procedure, inclusive of scanning, use of anesthesia or other medications, and intravenous contrast (gadopentetate dimeglumine). General anesthesia was used in 285 of the studies (21.4%), with 12 AEs in those patients (4.2%, $p = .001$).

There were 7 AEs (6.5%, $p = .001$) in 107 studies performed on hospitalized patients, the majority involving patients from the intensive care unit, 5 AEs (5.2%, $p = .018$) in 97 studies performed on patients under the age of 1 year, and 3 AEs (2.2%, $p = .479$) in 134 studies performed on patients with single ventricle physiology. Studies performed on inpatients under general anesthesia had the highest rate of AE (7 AEs in 65 studies; 10.8%, $p < 0.001$). By multivariate logistic regression analysis, use of anesthesia (OR 3.56 [95% CI 1.33, 9.56], $p = .012$) and inpatient status (OR 3.70 [95% CI 1.23, 11.1], $p = .020$) were significant predictors of AEs.

Conclusions: CMR in patients with congenital heart disease has a low rate of complications. Use of general anesthesia and examinations on hospitalized patients are independent risk factors for AEs. The patients at highest risk for AE were those inpatients who required anesthesia, with the majority of AEs in this group occurring in intensive care unit patients, highlighting that the most acutely ill patients are most at risk. Along with its well-established diagnostic utility, the safety profile of this test, including its avoidance of ionizing radiation, gives CMR a favorable risk-benefit profile for the diagnostic evaluation of the central cardiovascular system in this patient population.

302. IDENTIFICATION OF HYPERTROPHIC CARDIOMYOPATHY BY MAGNETIC RESONANCE IMAGING IN THE ABSENCE OF ECHOCARDIOGRAPHIC DIAGNOSIS

Carsten Rickers, MD,¹ Barry Maron, MD,² Michael Jerosch-Herold, PhD,³ Susan Casey, RN,² Hans H. Kramer, MD,¹ Prasad Panse, MD,⁴ Neeta Panse, MD,⁴ Andrey Zenovich, MSc,² Norbert Wilke, MD.⁵ ¹University Hospital Kiel, Kiel, Germany, ²Minneapolis Heart Institute Foundation, Minneapolis, MN, USA, ³Advanced Imaging Research Center, Portland, OR, USA, ⁴Health Science Center, University of Florida, FL, USA, ⁵Health Science Center, University of Florida, FL, USA.

Introduction: The two-dimensional echocardiogram (ECHO) has been the standard, noninvasive diagnostic test for the clinical diagnosis of hypertrophic cardiomyopathy (HCM) and also has an important role in risk stratification. A direct relation between magnitude of wall thickness and risk for sudden death has been demonstrated. We hypothesized that MRI would be more powerful than echo in establishing the diagnosis and measuring the extent of hypertrophy in HCM.

Methods: Forty-eight patients (age: 34 ± 16) suspected of (or known to have) HCM were imaged by both ECHO and MRI. With cine imaging 10–15, short axis slices (5–8 mm) were acquired to assess LV wall thickness. Standard LV cross-sectional views were obtained by Echo and compared to MRI. Maximum wall thickness was measured in 8 anatomic segments (anterior and posterior ventricular septum; anterolateral and posterior free wall) in both the distal and proximal LV; a total of 384 segments were assessed in 48 patients. Wall thickness measurements were made in a blinded fashion with ECHO and MRI.

Results: In 3 of 48 pts (6%) with a family history of HCM, Echo was judged normal without LV hypertrophy in any segment. However, MRI showed otherwise undetected hypertrophy in the anterolateral free wall (17 and 20 mm; twins age 14 and 19 mm; age 43) resulting in the phenotypic diagnosis of HCM for the first time and triggering implantation of cardioverter-defibrillator for primary prevention of sudden death in 2 of them. MRI more commonly showed the greatest LV thickness than did Echo (26 vs 16 pts; $p < 0.05$). Also, MRI identified LVH (undetected by echo) in 28 of 384 segments (7%) in 16 pts (33%). In 6 pts, echo was technically suboptimal and MRI made the diagnosis of HCM in (3 pts) or excluded it (3 pts).

Conclusions: MRI was advantageous over ECHO to: 1) definitively identify regions of LV hypertrophy not recognized by ECHO, and therefore was solely responsible for the identification of the phenotype in an important minority (6%) of pts; 2) enhance assessment of the magnitude of LV hypertrophy for the purpose of risk stratification and provides a diagnostic alternative for pts with technically inadequate Echo.

303. EVIDENCE FOR RIGHT VENTRICULAR INVOLVEMENT IN HYPERTROPHIC CARDIOMYOPATHY: A CMR STUDY

Martin S. Maron, MD,¹ James E. Udelson, MD,¹ Kraig V. Kissinger,² Lois Goepfert,² Warren J. Manning, MD.²
¹Tufts-New England Medical Center, Boston, MA, USA,
²Beth Israel Deaconess Medical Center, Boston, MA, USA.

Introduction: Hypertrophic cardiomyopathy (HCM) is the most common genetic cardiovascular disease with 12 sarcomeric protein mutations causing the characteristic phenotype of left ventricular (LV) hypertrophy. While abnormalities of the right ventricle have been recognized in HCM, the RV has been difficult to assess quantitatively using traditional non-tomographic imaging techniques such as 2D echocardiography and radionuclide ventriculography. Contemporary cardiovascular magnetic resonance imaging (CMR) techniques provide superior spatial resolution with complete 3-D, tomographic coverage of the entire heart. Therefore, it is timely to readdress the question of whether the RV is morphologically abnormal and a component of HCM.

Purpose: Abnormalities of RV mass and wall thickness are present in patients with HCM.

Methods: Cine CMR and a delayed enhancement (DE) CMR following the intravenous injection of 0.2mmol/kg Gd-DTPA

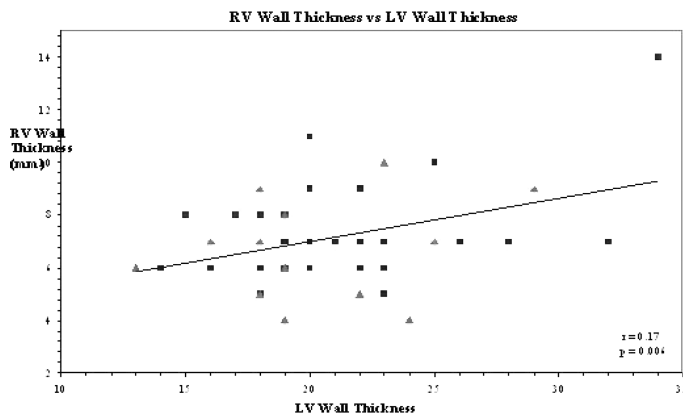


FIG. 1. Right ventricular wall thickness is plotted against left ventricular wall thickness. Triangles represent females and squares represent males.

were performed on 45 HCM patients (age 42 ± 16 years; 70% male) using a Philips Gyroscan ACS-NT 1.5T whole body CMR scanner. Contiguous (no gap) 10 mm thick short-axis breath hold cine images were acquired encompassing the entire right and left ventricle. On each short axis end-diastolic frame, the endocardial and epicardial borders of both the left and right ventricles were manually planimetered for mass and volume determination. On each end systolic frame, the endocardial borders were used for volume determination. On each short axis slice, the RV free wall was defined by a line connecting the RV cavity-interventricular septal junction with the epicardial RV free wall-interventricular junction. Care was taken to exclude epicardial fat and pericardium from the RV mass analysis.

Results: Maximum wall thickness of RV was 7.1 ± 1.9 mm and of LV was 20.7 ± 4.3 mm; values for absolute RV wall thickness greatly exceeded normal historical controls (3.8 ± 0.3 mm) (1). RV free wall mass was 53.5 ± 18.6 g compared to the LV mass of 192.1 ± 69.7 g. RV free wall mass also exceeded normal historical controls (44.6 ± 7.8 g). There were relatively weak ($r = 0.2$) although statistically significant correlations between RV and LV maximal wall thickness ($p = 0.0004$) and between RV and LV mass (Fig. 1; $r = 0.15$; $p < 0.0001$). One patient (2%) had substantial RV free wall hyperenhancement.

Conclusions: Our CMR data suggest that RV hypertrophy may be more common than previously recognized among patients with HCM. Further studies will be needed to assess the potential independent prognostic implication of RV pathology.

REFERENCE

- Am J Cardiol 1992; 69:1223–8.

304. MRI SUPERIOR TO PET AND SPECT FOR ASSESSMENT OF MYOCARDIAL VIABILITY IN A SMALL ANIMAL MODEL

Daniel K. H. Thomas, MD,¹ Harshali Bal, PhD,¹ Jim Horowitz, MD,¹ Paul Acton, PhD,¹ Bernd Misselwitz,

PhD,² Charles Dumont, MD,¹ Luis Araujo, MD,¹ Victor A. Ferrari, MD.¹ ¹University of Pennsylvania, Philadelphia, PA, USA, ²Schering AG, Berlin, Germany.

Introduction: Cardiovascular research involving small animal (SA) acute myocardial infarction (AMI) models relies increasingly on noninvasive imaging methods such as CMR. With greater availability, SA PET and SPECT may serve as alternatives to CMR for AMI imaging. Given the lack of available data on the relative performance of these tools, we performed the first direct comparison of these techniques for quantitative assessment of AMI.

Methods: Thirteen Sprague-Dawley-rats were imaged by CMR (4.7 T, Varian Inova) within 18–24 h post reperfused myocardial infarction (pMI). Within the next 18–24 h pMI MIBI-SPECT and FDG-PET were performed. Following SPECT/PET scanning, animals were sacrificed and their hearts stained with TTC (1.5% in PBS). Six additional rats were scanned with SPECT/PET to serve as normal controls. For CMR, a necrosis-specific contrast agent (Gadophrin-3) was injected at least 2h before imaging; parameters of the late enhancement (LE) sequence (FLASH) were: flip angle 60°, TR 6 ms, TE 3 ms, FOV 5–6 cm, matrix 128 × 128, reconstructed to 256 × 256, slice thickness 1.5 mm. This sequence acquires LE and functional images contemporaneously. The SPECT/PET images were acquired 1 h after the respective tracer injections. PET imaging was performed on a high resolution SA PET scanner (Philips Medical Systems, Cleveland, OH), using a 2 × 2 × 10 mm³ L-YSO Anger-logic detector, diameter = 21 cm, transverse field-of-view of 12.8 cm, axial length of 12.8 cm, and spatial resolution of 2 mm in the central region of the FOV. Images were reconstructed using the row action maximum likelihood algorithm. SPECT imaging

was performed on a Prism 3000XP triple-headed gamma camera (Philips Medical Systems, Cleveland, OH), equipped with custom-made tungsten knife-edge pinhole collimators (Nuclear Fields, Des Plaines, IL). The pinhole diameter was 3 mm, with spatial resolution of 3 mm. Acquisition parameters: continuous mode with 120 projection angles over a 360° arc to obtain data in a 128 × 128 matrix with a pixel size and slice thickness of 3.56 mm. Images were reconstructed using 10 iterations of an ordered-subsets expectation maximization (OS-EM) algorithm, with resolution recovery. Reconstructed images had an isotropic voxel size of 0.67 mm. For all techniques infarction-size was calculated as %LV-area.

Results: All infarcted animals (n = 13) completed the CMR and SPECT studies and all datasets were included in the study. Infarcted regions were detected on CMR images as an area with uptake of Gadophrin, whereas the corresponding regions on radionuclide images resulted in a decreased tracer-uptake (Fig. 1, row: 1a CMR, 1b SPECT, 1c PET; three representative short axis slices shown). One rat died 10 min after FDG-tracer injection. The PET data of 6 other animals could not be included due to increased FDG-uptake in the border zones, most likely reflecting stunned/hibernating myocardium, which precluded the quantitative analysis. Compared with SPECT and PET imaging, CMR revealed the greatest accuracy for detection of AMI, and showed the closest correlation and agreement with the TTC data (Fig. 2), followed by SPECT (Fig. 2) and PET (Fig. 2). In addition, the CMR datasets could be used to derive global left ventricular (LV) functional data in all rats.

Conclusion: We performed the first head-to-head quantitative comparison of CMR, PET, and SPECT for detection of AMI in a SA model. CMR was superior to the other modalities in delineating infarcted myocardium, due in large part to the greater

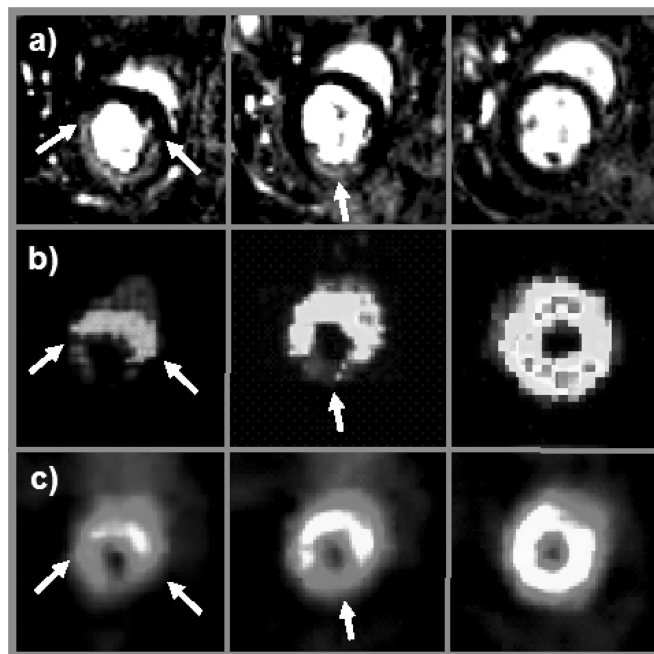


FIG. 1.

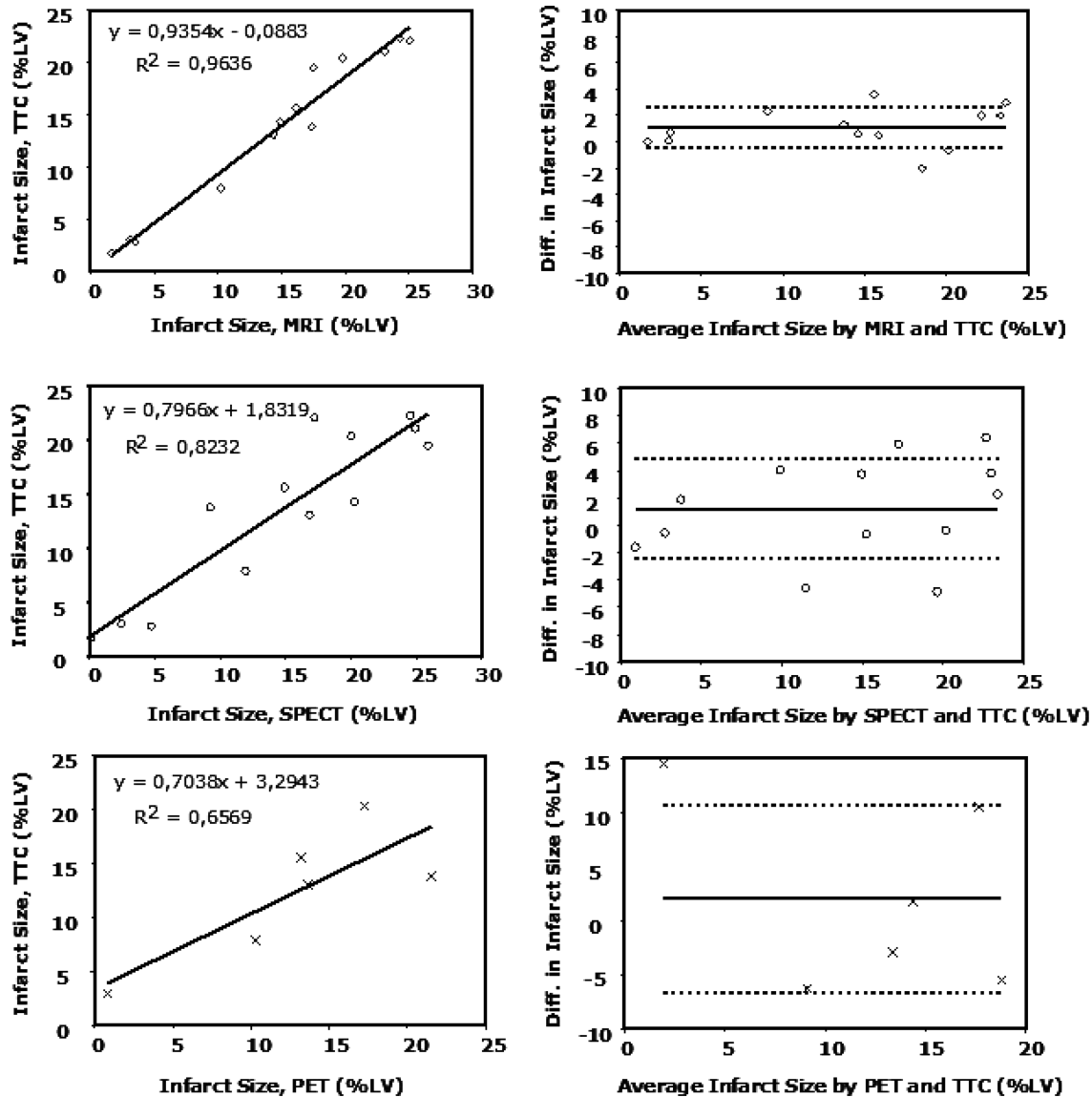


FIG. 2.

spatial resolution and the ability to detect necrotic myocardium. In addition, it was possible to derive complete global LV functional data from the same CMR datasets used for LE imaging. We noted an increased FDG-uptake in the border zones of AMI in some rats ($n = 6$), precluding quantitative analysis. This most likely reflects hypoperfused hibernating myocardium, but warrants further investigation.

305. RESPIRATORY NAVIGATOR GATED ^1H -MR SPECTROSCOPY OF THE HUMAN HEART TO ASSESS MYOCARDIAL TRIGLYCERIDE CONTENT: A STUDY ON REPRODUCIBILITY

Rutger W. vd Meer, MD,¹ Sebastian Kozerke, PhD,² Joost Doornbos, PhD,¹ Michael Schär, PhD,² Jeroen J. Bax, MD, PhD,¹ Albert de Roos, MD, PhD,¹ Hildo J.

Lamb, MD, PhD.¹ ¹Leiden University Medical Center, Leiden, The Netherlands, ²University of Zurich, Zurich, Switzerland.

Introduction: Triglyceride (TG) content of the liver and skeletal muscle, assessed with proton magnetic resonance spectroscopy (^1H -MRS), has been shown to be a valuable biomarker for metabolic disturbances both in animals and in humans. Myocardial TG content can be a marker of disease as well. However, ^1H -MRS of the human heart is difficult to perform due to respiratory and cardiac motion. Recently, respiratory motion compensation based on navigator echoes became available to improve spectral quality.

Purpose: To study the reproducibility of ^1H -MRS with respiratory navigator gating to assess myocardial TG content in the human heart.

Materials and methods: ¹H-MRS of the interventricular septum was performed in 21 healthy subjects (7 women, 14 men, age 19–54 years), at 1.5T. A 8 cm³ spectroscopic voxel was positioned in the septum, avoiding contamination from epicardial fat. A body coil was used for RF transmission and a surface coil for signal reception. A spectrum with and without water suppression was acquired in end-systole. The single-voxel spectra were recorded by using a point resolved spectroscopy sequence with an echo time of 26 ms and a repetition time of 2900 ms. 1024 data points were collected over a 1000 Hz spectral width and averaged over 128 acquisitions. Spectra without water suppression with a repetition time of 10s and with 4 averages were also recorded to be used as an internal standard. In addition, respiratory motion compensation based on navigator echoes was used to minimize breathing influences. Repeat scanning was performed the same session (intra-examination) with the same parameters and at two different occasions (inter-examination) an hour apart. Inter-examination scanning without respiratory gating was performed as well. Chemical shifts were measured relative to water at 4.7 ppm. TG signals at 1.3 and 0.9 ppm of the suppressed spectrum and the water signal of the unsuppressed spectrum were quantified using the MRUI/AMARES package. Finally the percentage of myocardial TG was calculated (TG/(water + TG) × 100).

Results: The intra-examination intraclass correlation coefficient (ICC) for the assessment of the percentage of myocardial TG was 0.97 (P < 0.05). Spearman’s rho correlation coefficient was 0.94 (P < 0.001). There was a coefficient of variance of 9.1%. Inter-examination ICC for the assessment of the percentage of myocardial TG with the use of respiratory motion compensation was 0.91 (P < 0.05). Spearman’s rho correlation coefficient was 0.80 (P < 0.001). There was a coefficient of variance of 17.6%. Inter-examination ICC for the assessment of the percentage of myocardial TG without the use of respiratory motion compensation was 0.24 (P > 0.05). Spearman’s rho correlation coefficient was 0.22 (p > 0.05). There was a coefficient of variance of 34.1%.

Conclusion: Respiratory navigator gated ¹H-MRS of the human heart showed good reproducibility to determine myocardial TG content. Reproducibility was substantially less without respiratory gating, thereby proving the importance of respiratory motion correction in ¹H-MRS.

306. QUANTITATIVE MYOCARDIAL PERFUSION AT 3T: COMPARISON OF REGIONAL FLOW RESERVES ACQUIRED IN LONG AND SHORT AXIS VIEWS

Christopher J. McGann, M.D., Nathan Pack, Henry Buswell, Edward Gilbert, M.D., Feras Bader, M.D., Edward V. DiBella, Ph.D. University of Utah, Salt Lake City, UT, USA.

Introduction: Myocardial perfusion reserve (MPR) is a non-invasive imaging correlate to coronary flow reserve and can be used to determine the presence of myocardial ischemia resulting

from coronary artery disease. Perfusion reserve can be estimated from the ratio of absolute myocardial blood flow (MBF) during hyperemia and resting states. Quantitative techniques in magnetic resonance (MR) perfusion imaging can accurately reflect MBF and MPR and has been shown to correlate with labeled microspheres (1). Here we use two compartment modeling to assess MPR at 3 Tesla (3T) using a single bolus technique with regional perfusion comparisons between acquisitions in short and long-axis views.

Purpose: We hypothesized that MR perfusion imaging at 3T will demonstrate close correlation between MPR values when flow data acquired in short versus long-axis views.

Methods: Study patients. Five subjects (3 men, 2 women; ages 30–68) underwent the vasodilator stress MR perfusion imaging protocol. This group included 2 normal volunteers and 3 patients with known non-obstructive CAD by recent coronary angiography. **Stress imaging technique.** Imaging was performed using a 3T Siemens Trio MR scanner with an eight channel phased array cardiac coil. Perfusion imaging was acquired with a 2D saturation recovery turboFLASH partial Fourier (74%) sequence at hyperemia (adenosine 140 ug/kg/min × 6 minutes) and at rest 15 minutes apart. The Gd-DTPA contrast agent was injected 6cc/sec via antecubital vein at stress and rest. Parameters include FOV 320–360 × 240–270, matrix 192 × 144, slice thickness 8 mm, TR 1.7 ms, TE 1.0 ms, TI 110 ms, flip angle 15°. Three short-axis slices and one 2- or 4-chamber long-axis slice were acquired each heartbeat for 80 R-R intervals. Perfusion data was corrected for coil sensitivity and motion. **Myocardial perfusion reserve (MPR).** Values for MPR were calculated from absolute MBF (ml/min/g) in four regions (anterior, inferior, inferior septal, and lateral walls) from both short and long-axis acquisitions with rest perfusion data corrected for rate pressure product. Perfusion data for posterior wall and anterior septum not evaluated as three chamber long-axis views were not acquired.

Results: Average corrected values for regional MPR are shown for short axis (SA) and long-axis (LA) views (Table 1) and were calculated from the ratios of regional MBF in each subject (Fig. 1). Hyperemia resulted in average global MPR 3.05 ± .03 in short-axis and 2.98 ± 0.3 in long-axis. In addition, regional values for MPR correlated closely in short and long-axis measurements within and between individual subjects. These results for MPR in non-ischemic subjects are similar to those established by perfusion imaging with positron emission tomography and MR studies at lower magnetic field strengths.

Conclusions: Results here suggest that quantitative MR per-

TABLE 1
Myocardial perfusion reserve

Region/Wall	SA	LA
Anterior	3.23 ± 1.1	3.13 ± 0.8
Inferior	3.32 ± 1.0	3.29 ± 1.0
Lateral	2.86 ± 0.7	2.75 ± 0.5
Septal	2.79 ± 0.5	2.78 ± 0.3
Average	3.05 ± 0.3	2.98 ± 0.3

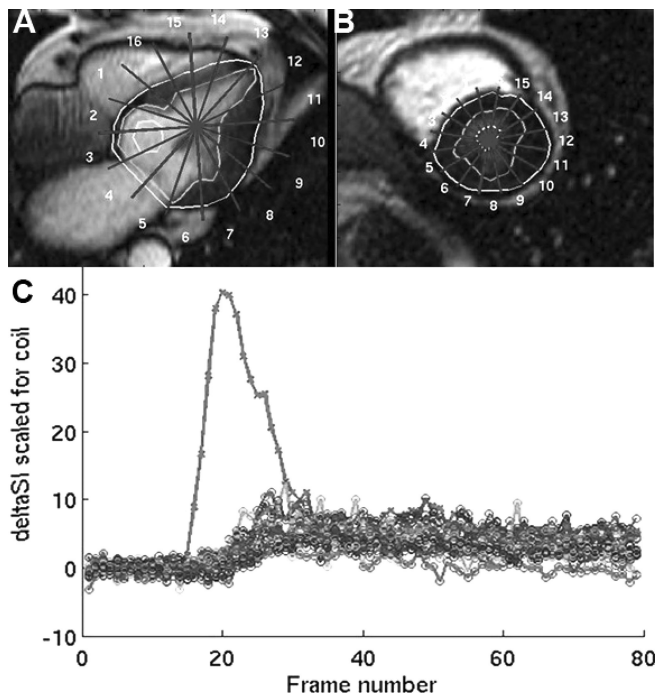


FIG. 1. Top panels show examples of 4-chamber long (A) and mid-LV short-axis (B) from which perfusion measurements are calculated. Lower panel (C) shows example of input function and issue residue curves for a given slice over 80 frames.

fusion imaging at 3T accurately reflects MPR in non-ischemic subjects. In addition, perfusion measurements in long-axis views correlated well with those from parallel short-axis views. Since long-axis imaging may have advantages in terms of extent of myocardial coverage and better delineation of basal and apical regions (2), it may be used as an alternative or adjunct to imaging in short-axis. However, trade-offs in resolution and out-of-plane motion imply a combination of selected short and long-axis views may be most useful.

REFERENCES

1. Christian, et al. *Radiology* 2004;232:677-84.
2. Wang, et al. *J Magn Reson Imaging* 2005;22:53-58.

307. CORRELATION OF WALL THICKNESS WITH LEFT VENTRICULAR MASS IN HYPERTROPHIC CARDIOMYOPATHY: IMPLICATIONS FOR SUDDEN DEATH RISK STRATIFICATION

Martin S. Maron,¹ James E. Udelson, MD,¹ Barry J. Maron, MD,² John R. Lesser, MD,² Andrey G. Zenovich, MSc,² Kraig V. Kissinger,³ Lois Goepfert,³ Warren J. Manning, MD.³ ¹Tufts-New England Medical Center, Boston, MA, USA, ²Minneapolis Heart Institute Foundation, Minneapolis, MN, USA, ³Beth Israel Deaconess Medical Center, Boston, MA, USA.

Introduction: The magnitude of left ventricular (LV) hypertro-

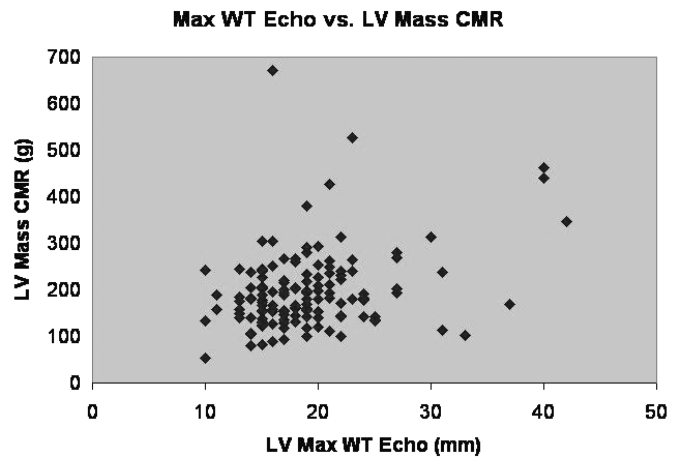


FIG. 1.

phy is an independent predictor of sudden cardiac death in hypertrophic cardiomyopathy (HCM), with extreme wall thickness (WT) ≥ 30 mm by echocardiography (echo) conferring the greatest risk (1). However, in contrast to the geometric assumptions used to derive LV mass by M-mode or two-dimensional echocardiography, CMR permits a true three-dimensional assessment of LV mass without the need for geometric assumptions and thus a more reliable assessment of magnitude of LV hypertrophy.

Purpose: LV wall thickness by echo will not closely define LV mass by CMR.

Methods: CMR and 2D guided M-mode echocardiography were performed on the same day in 144 HCM patients (age 42 ± 16 years; 70% male). The greatest thickness measured at any site within the LV wall represented maximum wall thickness. LV mass by CMR was calculated using a Simpson's Rule method from contiguous series of 10 mm thick slices (no gap) in the short axis plane and covering the entire LV, uncorrected for body size.

Results: There was a significant correlation between maximal LV wall thickness by CMR and echo ($p = 0.0001$), but CMR maximal LV wall thickness exceeded that of echo (20 ± 5 vs 18 ± 5 mm $p = 0.001$). Total LV mass by CMR was 198 ± 84 g (range 54-672 g) with a weak ($r = 0.3$; Fig. 1) but significant relationship between CMR LV mass and maximal LV wall thickness by echo ($p = 0.0002$). Among patients with extreme echo WT (≥ 30 mm), 3 of 8 (37%) had normal CMR LV mass (< 200 g). In contrast, 28 of 92 (30%) of patients with mild echo WT (≤ 19 mm) had greater than normal LV mass.

Conclusions: Though significant, there is only a weak correlation between echo maximal WT and global LV mass by CMR. Echo may overestimate overall LV mass relative to CMR when WT is extreme and underestimates when WT is mild. CMR measures of LV mass may prove to be a better marker of risk stratification for sudden death in HCM than wall thickness alone.

REFERENCE

1. NEJM 2000.

308. DETECTION OF EARLY SYSTOLIC DYSFUNCTION IN CARDIAC AMYLOIDOSIS WITH MYOCARDIAL TAGGING

Byoung Wook Choi, MD,¹ Susan B. Yeon, MD,¹ Connie Tsao, MD,¹ Kraig V. Kissinger, BS,RT(R)(MR),¹ Martha Skinner,² Warren J. Manning, MD,¹ Idith Haber, PhD,³ Fredrick Ruberg, MD.² ¹Beth Israel Deaconess Hospital, Boston, MA, USA, ²Boston University School of Medicine, Boston, MA, USA, ³Children's Hospital, Boston, MA, USA.

Introduction: Cardiac amyloidosis is a diffuse infiltrative process that impairs systolic and diastolic ventricular function. Unfortunately, disease detection often occurs late, when depression of global systolic function has ensued limiting treatment options. Abnormalities of longitudinal systolic contraction have been suggested by echocardiographic studies in patients with early-stage amyloid cardiomyopathy (AC) with normal fractional shortening (1). Therefore, detection of early systolic dysfunction by tagging methods sensitive to changes not apparent by global methods may be helpful in the early detection of amyloid cardiomyopathy.

Purpose: To detect the early systolic dysfunction in cardiac amyloidosis by using a cardiovascular magnetic resonance (CMR) tagging method.

Methods: Ten subjects with biopsy proven systemic AL amyloidosis with cardiac involvement (AC) were enrolled in the study. CMR with CSPAMM was performed in these patients and 3 controls without cardiac amyloid. CMR study (1.5T Philips Intera) included assessment of left ventricular (LV) mass and volumes using an SSFP imaging sequence. Spiral CSPAMM imaging was acquired at the mid left ventricular level in a short axis view. Percent minimal principal stretch (MPS, a measure of primarily circumferential shortening with lower numbers indicative of greater shortening) between end-diastole and end-systole was

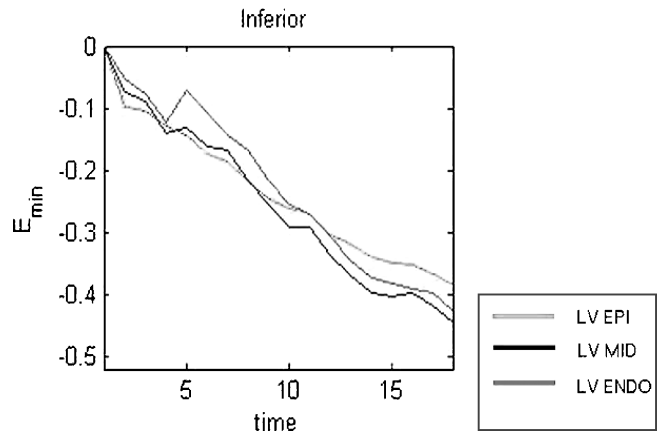


FIG. 2. "MPS-1" (E_{min}) during systole in a subject without cardiac amyloidosis demonstrating preserved circumferential in all three regions.

calculated for six myocardial segments in endocardial, middle, and epicardial layers using a customized local-phase based algorithm implemented in MATLAB. Two-sample t-tests were used to compare the results between cardiac amyloid subjects and healthy controls with a p-value < 0.05 considered significant.

Results: Cardiac amyloid subjects had a mean age of 58.7 ± 12.9 years and 8 (62%) were male. Control subjects had a mean age of 41 ± 14.4 years and 2 were male. CMR determined LV ejection fraction was similar (AC 62.3 ± 10.9 vs. control $64.3 \pm 3.2\%$; $p = .763$) but LV mass index was larger in the amyloid group (108.6 ± 31.8 vs. 54.0 ± 2.6 g/m²; $p = .00045$). However, mean MPS (averaged over all segments) in the AC group was greater than that in control group (0.74 ± 0.14 vs. $0.59 \pm 0.17\%$; $p = .00000003$) indicative of impaired circumferential shortening in the AC group. MPS values stratified by epicardial, middle, and endocardial myocardial regions in the AC group were significantly greater than those in the control group (0.81 ± 0.09 vs. $0.66 \pm 0.16\%$; $p = .0009$, 0.76 ± 0.12 vs. $0.58 \pm 0.18\%$; $p = .0008$, 0.67 ± 0.15 vs. $0.53 \pm 0.15\%$; $p = .0015$, respectively). MPS value in 5 of 6 segments in the AC group were significantly greater than those in the control group (anterior septum; 0.80 ± 0.09 vs. $0.68 \pm 0.11\%$; $p = .0099$; anterior; 0.71 ± 0.13 vs. $0.43 \pm 0.18\%$; $p = .0009$, anterolateral; 0.69 ± 0.12 vs. $0.48 \pm 0.17\%$; $p = .0062$, inferior; 0.81 ± 0.09 vs. $0.66 \pm 0.09\%$; $p = .0006$, inferior septal; 0.82 ± 0.09 vs. $0.74 \pm 0.07\%$; $p = .0082$).

Conclusions: In assessing functional deterioration due to cardiac amyloidosis, CMR tagging analysis may be applied to identify impairment of circumferential shortening that is not apparent by global measures of systolic function. This technique may facilitate the identification of amyloid cardiomyopathy at an early stage.

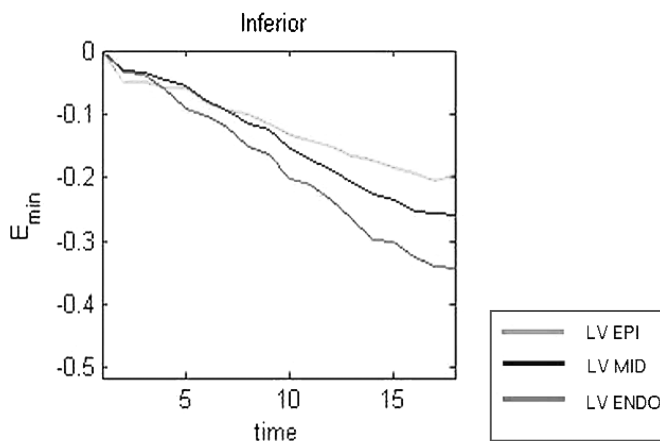


FIG. 1. "MPS-1" (E_{min}) during systole in the inferior segment of the mid left ventricle in a patient with cardiac amyloidosis. Decreased minimal principal stretch is noted in epicardial, mid, and endocardial layers.

REFERENCE

1. Koyama, et al. Circulation 2003.

309. CARDIAC MRI DURING SUSTAINED VENTRICULAR FIBRILLATION

Rajan D. Bhatt, MD, MBA, Vijayasree Kudithipudi, MD, Vincent Sorrell, MD. University of Arizona Medical Center, Tucson, AZ, USA.

Background: Most out-of-hospital ventricular fibrillation is prolonged (>5 minutes), and defibrillation from prolonged VF typically results in asystole or pulseless electrical activity. Each year over 600,000 people in the USA and Europe are victims of sudden cardiac arrest, commonly due to ventricular fibrillation. It is well known that the first 5 minutes of VF are the most critical for survival, yet what truly occurs during these first 5 critical minutes of sustained VF are not known. There are limitations within current imaging technology to acquire this data, but we have determined a new technique to bypass these barriers.

Methods: Ventricular dimensions were determined from magnetic resonance imaging for 30 minutes of untreated VF in a closed chest, closed pericardium model in six swine. Ungated steady-state free precession imaging from the base to the apex was performed (1). (See Berg [Sorrell] et al. *Circulation*. 2005;111:1136–1140 for details). We compared the rel-

ative changes of RV and LV volumes to relative changes in mid-ventricular single slice area over time.

Results: It was seen throughout 30 minutes of untreated VF that the RV and LV volumes correlated directly with the RV and LV mid-slice area, respectively. ($R^2 > 0.95$) (See Fig.).

Conclusion: Mid-slice area data can be used as a surrogate marker of prompt ventricular volume changes during VF and can be acquired 17 times faster than our previous method. Using this method, we plan to map out the physiologic changes during the first 5 critical minutes of VF.

REFERENCE

1. Berg, Sorrell, et al. *Circulation* 2005;111:1136–40.

310. ROBUST MULTI-SLAB WHOLE HEART IMAGING FOR REDUCED SENSITIVITY TO RESPIRATORY DRIFT AND HEART RATE VARIABILITY

Maggie M. Fung, MSc,¹ Wei Sun, PhD,² Thomas K. Foo, PhD,³ SuiHui Chen, MD,⁴ Naoyuki Takei, MSc.⁵ ¹GE

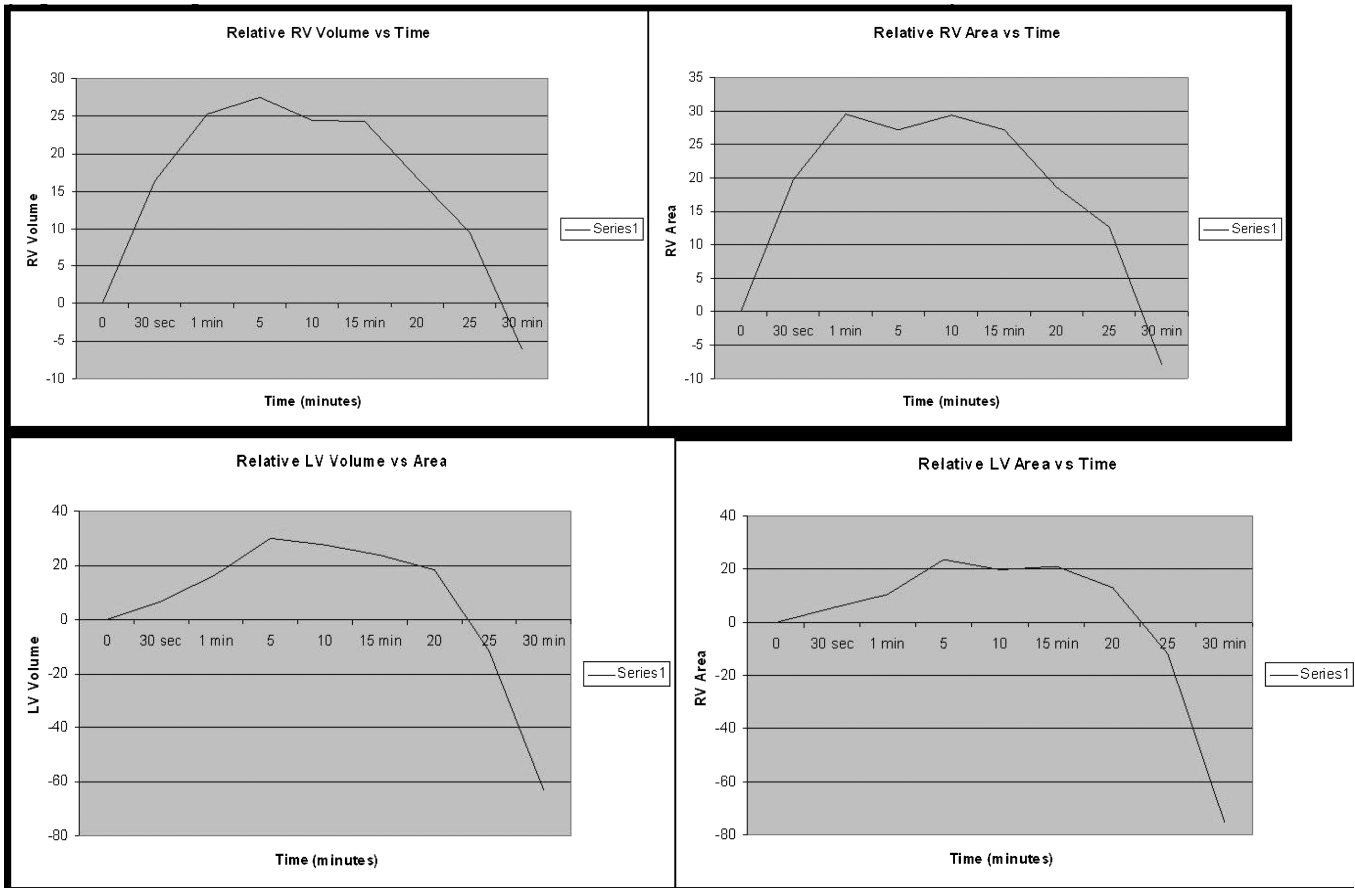


FIG. 1. % change of RV and LV volume and area over time. Time 0 = induction of VF.

Healthcare, Baltimore, MD, USA, ²GE Healthcare, Beijing, China, ³GE Global Research Center, Niskayuna, NY, USA, ⁴Chinese PLA General Hospital, Beijing, China, ⁵GE Healthcare, Hino, Japan.

Introduction: Whole heart imaging techniques has been developed for comprehensive assessment of coronary artery disease. However, during the long scan time required in a high spatial resolution whole heart free-breathing acquisition, variations in respiratory pattern and heart rate are often observed. They degrade image quality and respiratory drift often leads to prolonged scan time.

Purpose: This study seeks to demonstrate a whole heart acquisition strategy that i) reduces the impact of respiratory and cardiac motion variation on image quality, and ii) increases the success rate of free-breathing whole heart imaging. We proposed a multi-slab whole heart acquisition technique that divides a single volume into several thinner adjacent slabs, thus reducing the motion variability within each slab.

Methods: Multiple overlapping slab whole heart acquisition was performed in 7 healthy volunteers on a 1.5T GE HD whole body system (PLA, Beijing, China) using an 8-element cardiac phased array coil (GE Healthcare, Waukesha, WI, USA). A multi-slab 3D fat suppressed SSFP free-breathing sequence with T2-prep was used to acquire high spatial resolution non-contrast enhanced whole heart images (FA = 65, TR/TE = 4.6/2.0, 1 NEX, interpolated spatial resolution = $0.6 \times 0.6 \times 1 \text{ mm}^3$, cardiac acquisition window = 130 ms (HR > 80 bps) – 160 ms (HR ~ 60–80 bps)). The following parameters were selected to achieve the corresponding goals:

1. 4–5 slabs (16 slices per slab) were prescribed to ensure full heart coverage (Fig. 1).
2. 3 overlapped slices between adjacent slabs were used to reduce the signal reduction across slab boundaries
3. 16 slices per slab to limit the scan duration of each volume to 3–5 minutes and maximize the overall scan efficiency considering the ratio between overlapping and non-overlapping slices. The multi-slab acquisition strategy was compared with a conventional, single volume approach.

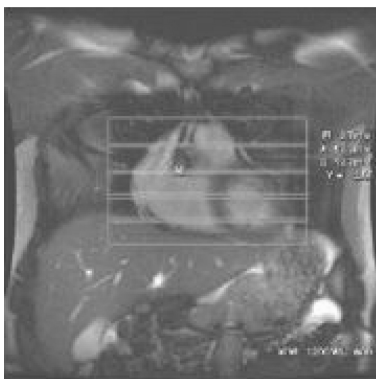


FIG. 1. Multi-volume whole heart acquisition technique.

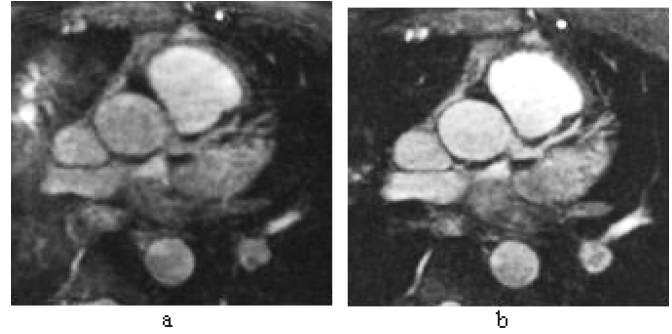


FIG. 2. LCA images (MIP) obtained from a healthy volunteer using a (a) single volume and (b) multiple slab whole heart acquisition. Scan duration of single volume was around 16–20 minutes while that of multiple slab scan was around 4 minutes per slab (total scan time ~16–24 minutes). Note the substantial improvement in delineation of the LCA achieved with multiple slab acquisition due to reduced respiratory pattern and heart rate variation.

Results: Improved cardiac and respiratory motion suppression were observed using the proposed multi-slab technique when compared to single volume approach (Fig. 2). With the multi-slab approach, the mean scan time was 3–5 minutes per slab compared to 15–20 minutes in the single large volume approach. This reduced image blurring due to variations in heart rate and respiratory patterns, yielding improved vessel delineation and reduced respiratory artifacts. The total scan time of the multi-slab approach was 15–20% longer than that of the single large volume approach due additional overlapping slices. However, as images were reconstructed and displayed to the user after the completion of each volume, the multi-slab approach had the advantage of assessing the image quality earlier and allowed user to re-acquire the scan if the image quality was not satisfactory. We observed that in cases where the single volume acquisition had to be terminated as the respiratory pattern shifted away from the end-expiratory window over time, multi-slab approach was minimally affected and was able to generate images with reasonable image quality. This was due to a smaller respiratory



FIG. 3. Planar reformation images showing the RCA (MIP) from a healthy volunteer using a multiple slab acquisition. The Venetian blind effect is minimal and does not affect the calibre of the vessel.



FIG. 4. 3D volume rendering whole heart acquisition obtained from multiple volume technique. LAD and LCA were clearly visualized.

positional shift within each sub-slab. The Venetian blind artifact associated with multiple overlapping slabs (MOTSA) was reduced to an imperceptible minimum. Increasing the number of overlapped slices at the expense of scan efficiency can further minimize this artifact but we found that 3 overlapping-slice was a reasonable compromise between image quality and scan efficiency (Fig. 3).

Discussion: It has been demonstrated that the proposed multi-slab acquisition strategies can reduce the impact of respiratory and cardiac motion variation on image quality and improve the success rate of whole heart acquisition in a clinical setting, where respiration and cardiac motion variation are more prominent in patient. This approach can be integrated with parallel imaging techniques in the future to increase the scan efficiency and further reduce the impact of heart rate variability and respiratory drift.